Energy level offset at organic semiconductor heterojunctions

A. Rajagopal, C. I. Wu, and A. Kahn

Citation: Journal of Applied Physics **83**, 2649 (1998); doi: 10.1063/1.367027
View online: http://dx.doi.org/10.1063/1.367027
View Table of Contents: http://scitation.aip.org/content/aip/journal/jap/83/5?ver=pdfcov
Published by the AIP Publishing

Energy level offset at organic semiconductor heterojunctions

A. Rajagopal, C. I. Wu, and A. Kahn[a)]
Department of Electrical Engineering, Princeton University, Princeton, New Jersey 08544

(Received 23 September 1997; accepted for publication 20 November 1997)

We present an investigation via ultraviolet photoemission spectroscopy of the electronic structure of three organic-organic heterojunctions formed between the standard electron-transport emissive material tris(8-hydroxy-quinoline)aluminum (Alq_3) and two hole-transport materials, i.e., 3,4,9,10 perylenetetracarboxylic dianhydride (PTCDA), and N,N'-diphenyl-N,N'-bis(l-naphthyl)-1-1′biphenyl-4,4″diamine (α-NPD). We measure directly the energy offsets between highest occupied molecular orbitals during the formation of the interfaces. We show that the relative positions of the highest occupied and lowest unoccupied molecular orbitals across the Alq_3/PTCDA and Alq_3/α-NPD interfaces are qualitatively different and explain, in part, the difference in the performance of electroluminescent devices based on these heterojunctions. We demonstrate the existence of charge transfer-induced dipoles which shift the molecular levels of one organic with respect to the other and invalidate the usual assumption of vacuum level alignment across organic heterojunctions. Finally, we show that the molecular level alignment is independent of the deposition sequence of the organic films and that transitivity applies to these organic ''band offsets.'' © *1998 American Institute of Physics.* [S0021-8979(98)04505-8]

I. INTRODUCTION

A considerable amount of work has been devoted in the past decade to the development of multilayer organic light emitting devices (OLEDs).[1] These structures generally comprise two contacts and at least one organic heterojunction between a hole transport (HT) layer and an electron transport (ET) layer. Holes are injected from a high work function anode into the HT layer and electrons are injected from a low work function cathode into the ET layer.[2,3] The electron-hole capture, exciton formation, and radiative recombination occur in the emissive layer near the organic heterojunction. Three-layer device structures where the emission takes place in a layer sandwiched between the HT and ET layers have also been demonstrated.[4]

The turn-on voltage and efficiency of OLEDs depend on many factors, in particular the characteristics of the contacts to the HT and ET layers, which control the balance of electron and hole currents injected in the device, and the transport of carriers in the organic layers and across the heterojunction. If the ET layer is also the emissive layer, the heterojunction should be designed to facilitate hole injection from the HT into the ET layer and to block electron injection in the opposite direction in order to enhance the probability of exciton formation and recombination in the emissive layer. By analogy to inorganic heterojunctions, hole injection into the ET layer is easy when the highest occupied molecular orbital (HOMO) of the HT layer at the interface is at the same energy as or below that of the ET layer. Conversely, electrons are confined in the ET layer when the lowest unoccupied molecular orbital (LUMO) at the interface is lower than that of the HT layer. An accurate determination of the electronic structure of organic heterojunctions is therefore essential for designing devices with optimum characteristics.

A key advantage of organic molecular semiconductors is that materials can be chosen out of a large pool of molecules in order to meet the device requirements. Structure is not an issue. The van der Waals intermolecular bonds are weak enough to allow structural flexibility without the penalty of defect formation. In particular, recombination centers, generally associated with broken covalent bonds at inorganic interfaces, presumably do not exist at organic interfaces. This relaxes the stringent conditions of lattice matching and defect-free interfaces required at inorganic heterojunctions. Organic heterojunctions can therefore be optimized through a judicious choice of materials chosen solely on electronic and transport criteria rather than through the more restrictive optimization of the growth and doping characteristics of a fixed set of crystalline materials used in inorganic devices.

Choosing organic materials to meet the interface characteristics described above is generally done by representing the heterojunction in a traditional ''band offset'' picture using the ionization energy (IE) and electron affinity (EA) of the materials, and assuming vacuum level (E_{vac}) alignment at the interface [Fig. 1(a)]. Surface and interface electronic states and charge transfers are neglected. The chief argument in favor of such a simplification, aside from a complete lack of detailed information about these interfaces, is that organic-organic interfaces are expected to be chemically and structurally simple because of the weak van der Waals intermolecular forces. These interfaces are construed as boundary layers between nearly noninteractive solids. There are, however, several problems with this simple approach. First, the IEs and EAs used for modeling the interface electronic structure are generally obtained by methods like electrochemical measurements[5] which do not reflect the conditions prevailing during formation of thin films. Second, the impact of the

a)Corresponding author; Tele: 609-258-4642; Fax: -6279; Electronic mail: kahn@ee.princeton.edu

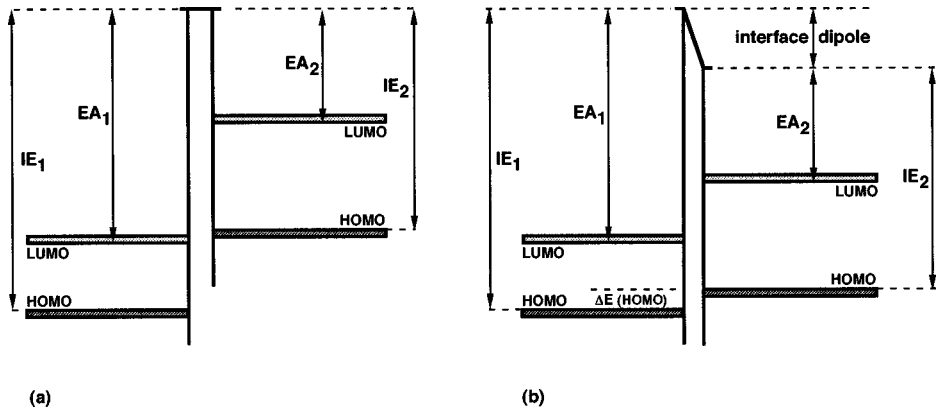

FIG. 1. Band structure representation of an organic heterojunction showing relative positions of HOMOs and LUMOs with (a) vacuum levels aligned across the interface and (b) an interface dipole. The ionization energies and electron affinities are shown.

physical perturbations caused by overlayer formation on the work function and IE of the materials is neglected. Third, charge redistribution and interface dipoles, which can shift the molecular levels of one solid with respect to the other [Figure 1(b)], are neglected. The initial assumption of E_{vac} alignment can therefore lead to errors in the relative positions of molecular levels and, consequently, in predictions of the electrical behavior of interfaces. There is no theoretical framework analogous to that developed for inorganic heterojunctions[6] to model organic heterojunctions. Transport mechanisms in organic molecular solids appear to be material-dependent and are not as well understood as in inorganic semiconductors. Using transport data to model the interface electronic structure is, at this point, uncertain at best. There is therefore a pressing need for accurate and direct determination of the electronic structure of organic interfaces via spectroscopic measurements of molecular level offset.

X-ray photoemission spectroscopy (XPS) and ultraviolet photoemission spectroscopy (UPS) have been and continue to be among the most important tools for investigating the chemistry and electronic properties of interfaces, in particular energy band offsets at semiconductor heterojunctions. The short probing depth of these techniques is ideally suited for *in situ* investigations of layer-by-layer formation of interfaces through direct measurement of interface bonding and energy level offset. Recently, an increasing number of photoemission studies on metal-organic interfaces have started to link interface chemistry and morphology to electronic structure and electrical characteristics of these contacts,[7–11] but only very few similar studies of organic heterojunctions have been published so far.[12,13] We report here a UPS investigation of heterojunctions formed between three small molecule organic semiconductors used in OLEDs: 3,4,9,10 perylenetetracarboxylic dianhydride (PTCDA), tris(8-hydroxy-quinoline)aluminum (Alq_3), and N,N'-diphenyl -N,N'-bis(l-naphthyl)-1-1′biphenyl-4,4″diamine (α-NPD) (Fig. 2). PTCDA and α-NPD are HT materials whereas Alq_3 is an ET material. We determine the molecular level offset at Alq_3/PTCDA, Alq_3/α-NPD, and PTCDA/α-NPD interfaces obtained through both deposition sequences. We demonstrate the existence of interface dipoles which invalidates the assumption of E_{vac} alignment at organic heterojunctions. We determine in each case the HOMO offset and discuss the impact of these electronic structures on the electroluminescence efficiencies obtained with the Alq_3/PTCDA and Alq_3/α-NPD pairs. Finally, we establish the transitivity of molecular level offset for these organic semiconductors.

II. EXPERIMENT AND METHODOLOGY

The measurements are performed in an ultrahigh vacuum system consisting of an analysis chamber (base pressure$=10^{-10}$ Torr) and an organic deposition chamber. The analysis chamber includes a UPS setup consisting of a He discharge lamp and a double-pass cylindrical mirror ana-

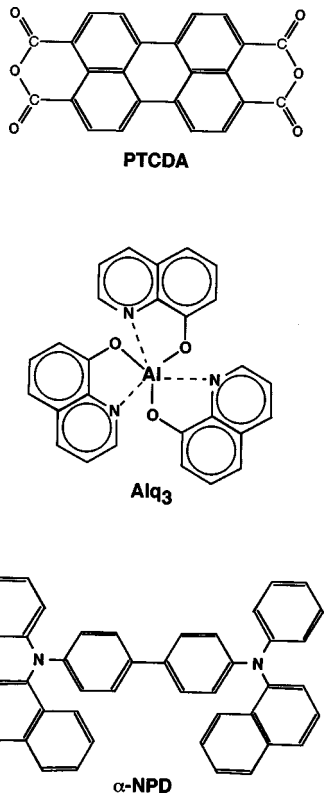

FIG. 2. Chemical structures of small molecules used in this work.

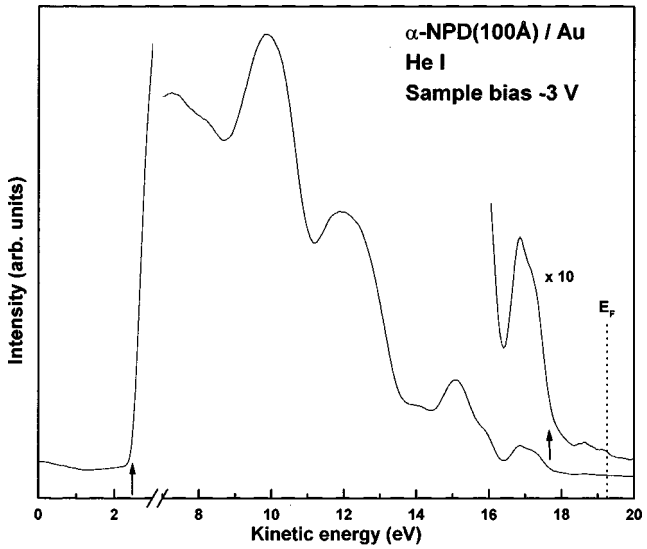

FIG. 3. UPS spectrum from a 100 Å thick film of α-NPD deposited on gold. The Fermi level E_F is measured on the gold substrate. Arrows indicate the top of the HOMO and the onset of photoemission. The sample is biased at -3 V.

lyzer. The resolution of the photoemission measurements is 0.15 eV. The organic deposition chamber (base pressure$=5\times10^{-10}$ Torr) is equipped with evaporation stations and a quartz microbalance. The organic materials are first purified *ex situ* by several cycles of vacuum sublimation, then placed in vacuum in effusion cells and thoroughly degassed. Typical evaporation temperatures range from 200 to 250 °C, giving deposition rate of a few monolayers per minute. Densities used for PTCDA, Alq_3, and α-NPD are 1.69, 1.55, and 1.55 g cm^{-3}, respectively. The pressure in the organic chamber during deposition ranges between 10^{-9} Torr for PTCDA and 10^{-8} Torr for Alq_3 and α-NPD. The substrates are gold films deposited on silicon wafers and are kept at room temperature during deposition.

UPS spectra from 100 Å thick films of each organic material are first recorded to determine the IE and the valence band line shape. IE is defined as the energy difference between $E_{\rm vac}$, measured by linear extrapolation of the low kinetic energy onset of the photoemission spectrum, and the top of the occupied states, measured by linear extrapolation of the high kinetic energy side of the HOMO peak. The photoemission onset is measured with the sample biased at -3 V to clear the detector work function. The electron affinity (EA) is defined as IE minus the optical band gap. UPS spectra, including onsets, are recorded for each heterojunction for increasing overlayer thickness ranging from the monolayer to about 30 Å, enough to produce a bulklike spectrum and bury the substrate signal without causing any noticeable charging. Both deposition sequences are used for each heterojunction.

The energy offset between substrate and overlayer HOMOs is determined for each interface and each deposition sequence. For the Alq_3/PTCDA interface, the similarity between the valence state line shape of the two organics and the relatively small offset between the two HOMOs requires a decomposition analysis using a least-square fitting routine.

TABLE I. Optical gap, ionization energy (this work), electron affinity (difference between first two columns), and position of the Fermi level with respect to the top of the HOMO for each thin film grown on gold.

	Optical gap (eV)	IE (eV)	EA (eV)	E_F-HOMO (eV)
PTCDA	2.2	6.8	4.6	1.8
Alq_3	2.7	5.95	3.25	1.9–2.1
α-NPD	3.1	5.7	2.6	1.7

This standard routine simultaneously subtracts the background and adjusts the position and intensity of the various peak components. Details on the parameters and method used to model the PTCDA and Alq_3 HOMO peaks have been given elsewhere.[7] For Alq_3/α-NPD and PTCDA/α-NPD, line shape differences are sufficient to permit a direct determination of the HOMO offset using fixed energy references to prominent valence band peaks. In all cases, the offset is determined for an overlayer thickness small enough that ''band bending'' could be totally neglected.

III. RESULTS

A. Single organic films

A UPS spectrum of the valence states of a 100 Å α-NPD film is shown in Fig. 3. The Fermi level (E_F) is measured on the gold substrate. The spectrum consists of a series of well defined peaks which are typical of molecular levels and reflect mostly π-orbitals at low binding energy and increasing

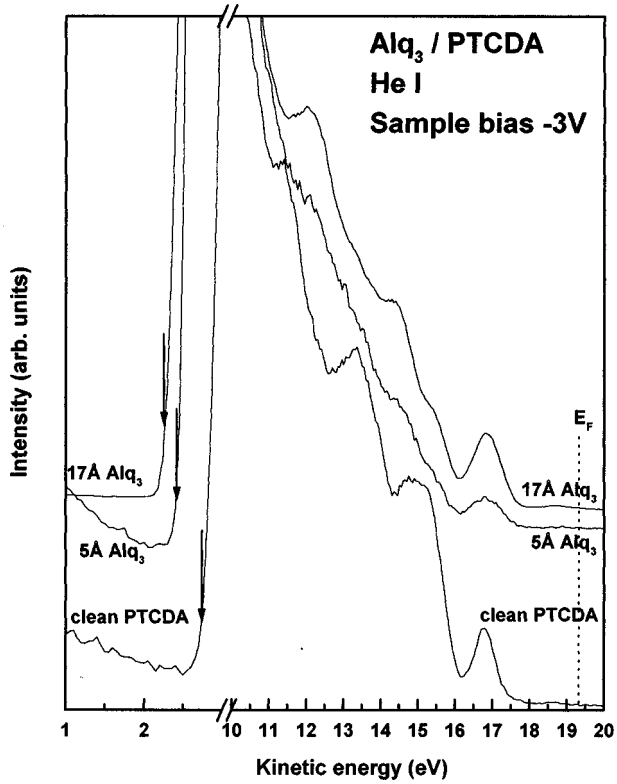

FIG. 4. UPS valence band spectrum from clean PTCDA and PTCDA covered with an incremental amount of Alq_3. The photoemission onset is indicated in each case by an arrow. Each spectrum is recorded with a -3 V bias on the sample.

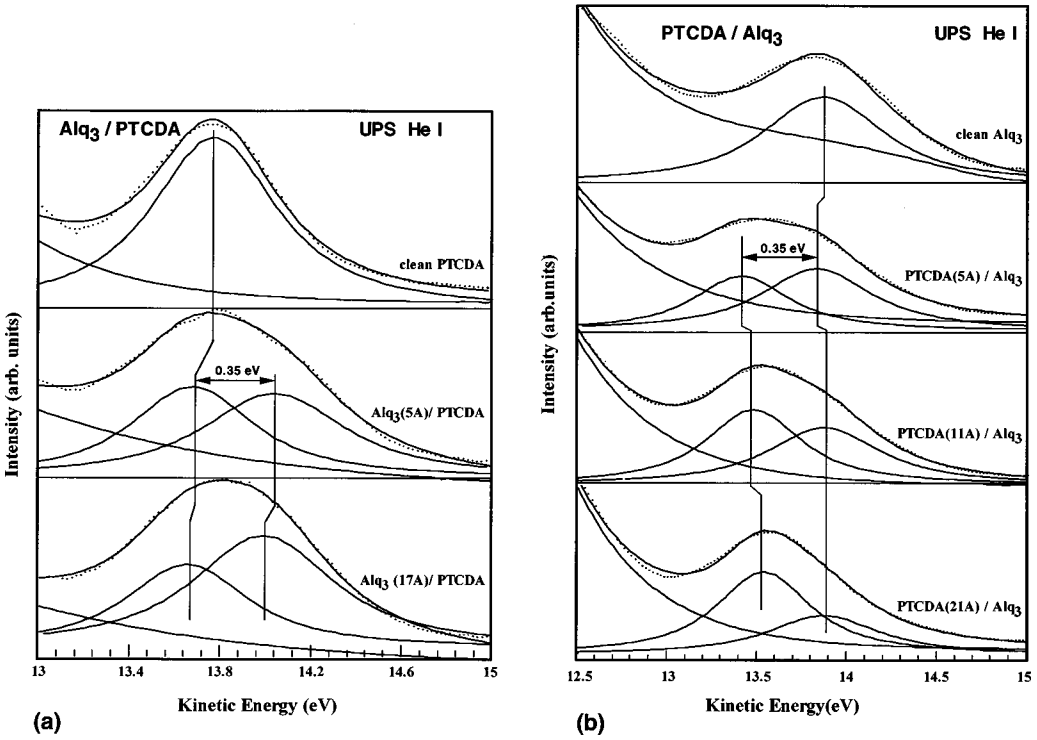

FIG. 5. Decomposition of the composite HOMO peak into PTCDA and Alq_3 components. The decomposition parameters are detailed in Ref. 12.

σ-like character at higher binding energy. The photoemission onset and the top of the HOMO are indicated by arrows. The IE of the three organics used in this work are summarized in Table I. The PTCDA value is about 0.5 eV higher than previously reported[14,15] whereas the Alq_3 value is in excellent agreement with previous data.[16] No spectroscopic data have been previously reported for α-NPD. It is worth noting that PTCDA and α-NPD, both HT materials, exhibit widely different electronic characteristics. The IE of PTCDA is 1.1 eV larger than that of α-NPD, whereas its optical band gap is 0.9 eV smaller. The EA of the two materials differ therefore by 2 eV (4.6 eV for the former, 2.6 eV for the latter).

The organic films are deposited on gold surfaces which have a work function $\phi_{Au}=5.2\pm0.1$ eV. They are 100 Å thick and undoped, and cannot sustain substantial band bending at equilibrium. Thus, the position of the top of the HOMO measured at the surface of the film (Table I) can be assumed to be the same (±0.1 eV) with respect to E_F throughout the organic film, i.e., ''flat band'' condition, and to correspond to the position at the organic/(gold)substrate interface. This is verified by the good agreement with positions measured in *interface* measurements, i.e., with only few monolayers of organics, for Alq_3/Au (1.8 eV) and α-NPD/Au (1.6 eV).[17] If the Schottky–Mott model was applicable to these interfaces, the PTCDA, Alq_3, and α-NPD HOMO should be at IE$-\phi_{Au}$, or 1.6, 0.75, and 0.5 eV, below E_F, respectively. The fact that the Alq_3 and α-NPD numbers presented in Table I depart drastically from this prediction indicates that interface states and dipoles are present and play a major role in the interface electronic structure, in agreement with the conclusions of recent investigations of metal/organic interfaces[18] and with those reached below. Interface molecules in a different configuration than in the bulk, bound to substrate atoms and eventually damaged by chemical reactions, could accept or donate charges and play the role of localized gap states.

B. Heterojunctions

1. Alq_3/PTCDA

Figure 4 shows the UPS spectra for clean PTCDA and PTCDA incrementally covered with Alq_3. The right-hand part of each spectrum corresponds to the valence band and HOMO, and the left-hand part corresponds to the onset of photoemission. The line shape of the spectrum changes with increasing amounts of Alq_3. Due to the short inelastic mean free path of the UPS electrons, the 17 Å spectrum is found to be identical to a spectrum from thick Alq_3. The 5 Å spectrum corresponds to a superposition of PTCDA and Alq_3 features. In particular, the 5 Å HOMO peak is substantially broadened by the superposition of the PTCDA and Alq_3 HOMO peaks shifted with respect to each other.

The decomposition of the HOMO peak using the least-square routine is shown in Fig. 5. The peak consists of two components: a PTCDA peak which shifts by 0.1 ± 0.05 eV toward lower kinetic energy with respect to the clean PTCDA HOMO peak; and an Alq_3 peak offset by 0.35 ± 0.05 eV toward higher kinetic energy with respect to the PTCDA peak. The change in the ratio of the two components is consistent with the increasing Alq_3 coverage. The same offset is obtained for the reverse interface, i.e., PTCDA/Alq_3, as has been described elsewhere.[12] The transition between the PTCDA spectrum and the Alq_3 spectrum is also marked by a 0.5 ± 0.05 eV shift of the onset toward

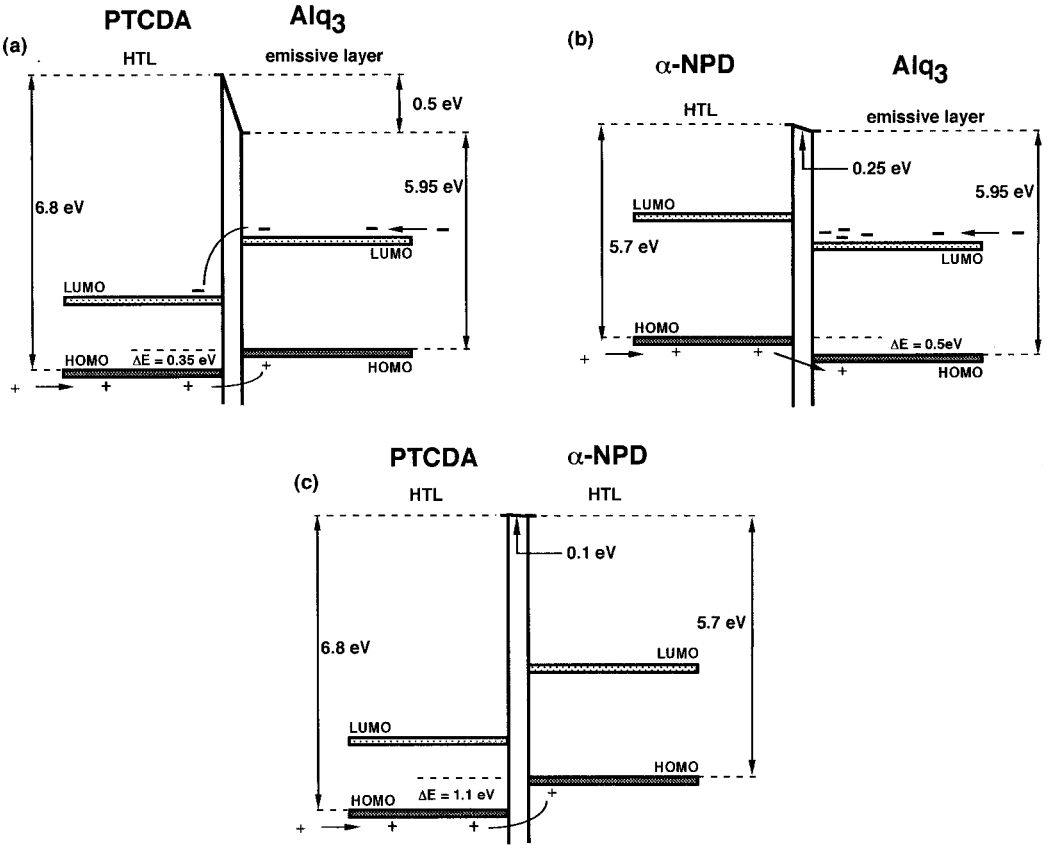

FIG. 6. Schematic of the (a) Alq_3/PTCDA (b) Alq_3/α-NPD, and (c) α-NPD/PTCDA interface electronic structure showing molecular level offset and interface dipole. Molecular levels are represented with an arbitrary small width.

lower kinetic energy, marking a corresponding lowering of E_{vac}. Again, the reverse deposition sequence leads to a shift with exactly the same magnitude, but opposite sign. The assumption of vacuum level alignment at the PTCDA/Alq_3 interface is therefore clearly invalid. A schematic representation of the interface molecular level alignment is given in Fig. 6(a).

2. α-NPD/Alq_3

Figure 7 shows the UPS spectra recorded upon incremental deposition of α-NPD on Alq_3. As in the previous case, the 4 Å spectrum displays a superposition of features from both organic materials. The 10 Å still shows a small distortion of the HOMO peak, and 20 Å spectrum is identical to that of thick α-NPD.

The offset between the α-NPD and Alq_3 HOMOs is determined in two ways: (1) by direct comparison of the linear extrapolations of the top of the HOMO on the substrate and on the 20 Å film; (2) by measuring the energy difference between the prominent peaks at about 10 eV below E_F and the top of the HOMO on thick films and comparing their relative position at the interface. Both methods lead to the same offset of 0.5 ± 0.05 eV with the α-NPD HOMO above that of Alq_3. The interface obtained by reversed deposition sequence leads to the same offset. No evidence of overlayer-induced band bending at the substrate surface is observed in either case. Finally, the photoemission onset shows a 0.25 ± 0.05 eV rise of E_{vac} from Alq_3 to α-NPD. The reverse

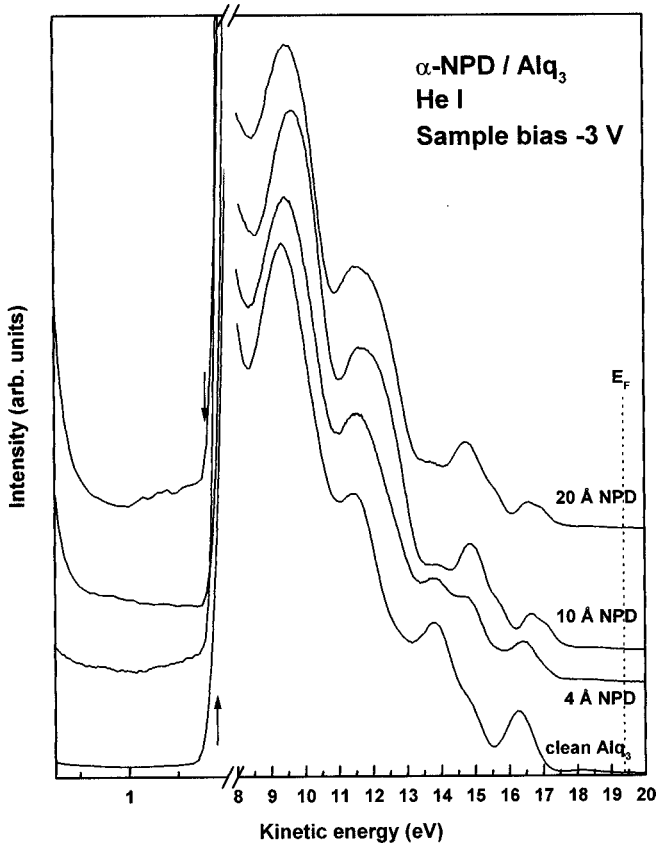

FIG. 7. Same as Fig. 4 for α-NPD/Alq_3. Only the onset of the Alq_3 substrate and of the 20 Å α-NPD layer are indicated by arrows.

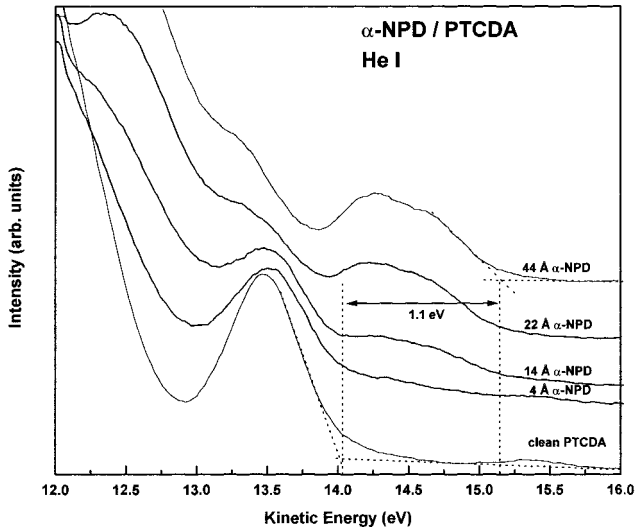

FIG. 8. Top of the valence band, including HOMO peaks, for α-NPD deposited on PTCDA.

deposition sequence leads to a comparable lowering of E_{vac}. Although this shift is smaller than in the previous case, it confirms that E_{vac} alignment is not a valid assumption for these interfaces. A schematic of the molecular level alignment is given in Fig. 6(b).

3. α-NPD/PTCDA

This last interface involves two HT materials with the largest IE and EA difference within the series. Figure 8 shows the expanded top of the valence band as a function of α-NPD coverage on PTCDA and the evolution from the single PTCDA HOMO peak to the double α-NPD HOMO peak. The offset is determined by extrapolation of the top of the corresponding peaks. Again, no overlayer-induced band bending is observed. The offset is 1.1 ± 0.05 eV with the α-NPD HOMO above that of PTCDA for both α-NPD/PTCDA and PTCDA/α-NPD interfaces. In both cases, the shift of the photoemission onset is surprisingly small, i.e., $\leqslant 0.1$ eV, and cannot be unambiguously established because of experimental uncertainty. The molecular level alignment is shown in Fig. 6(c).

IV. DISCUSSION

The electronic structures of the heterojunctions presented above are independent of the deposition sequence, at least within experimental resolution. Symmetry does not generally prevail at covalently bonded inorganic interfaces where overlayer-induced changes in surface structure, formation of defects and, more generally, interface chemistry depend sensitively on the deposition conditions and affect the interface electronic structure. The same is true for metal/organic interfaces. The evaporation of metal atoms from hot sources onto molecular surfaces causes far more defects and interdiffusion and leads to different electronic properties than the reverse deposition sequence. However, the interfaces investigated here are dominated by van der Waals intermolecular bonds. The heats of adsorption and kinetics involved with the deposition of molecules sublimated at low temperature

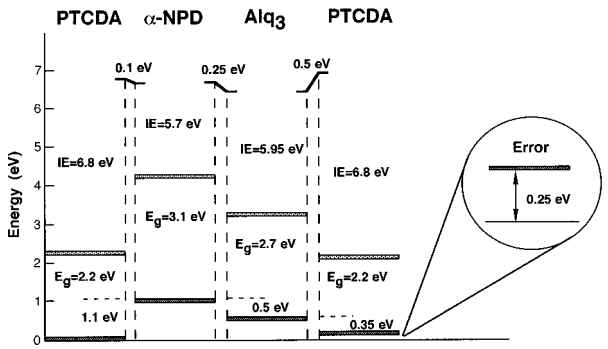

FIG. 9. Summary of molecular level offsets and dipoles across the three interfaces demonstrating transitivity.

($\sim 200-250\,^{\circ}\mathrm{C}$) on a molecular surface are far smaller than in inorganic systems. The deposition sequence is therefore not expected to have a significant impact on the interface electronic properties, and we indeed show in Fig. 9 that the molecular offset is transitive throughout the three heterojunctions and the deposition sequences. The 0.25 eV error results in most part from limited experimental resolution.

All the molecular level offsets reported in Fig. 6 correspond to staggered band gap configurations. The LUMO offsets should be considered as tentative, given that the LUMO position is deduced from the HOMO position by adding the optical gap. This procedure is not strictly valid, as it neglects issues of exciton binding energy and correlation effects in these molecular solids.[19] Nevertheless, the relative positions of the LUMOs are believed to be qualitatively correct.

The Alq_3/PTCDA and Alq_3/α-NPD heterojunctions exhibit a fundamental difference. Both junctions are between an ET layer (Alq_3) and an HT layer. Yet, in the former case, the Alq_3 HOMO and LUMO are higher than those of the HT layer, and in the latter, lower than those of the HT layer. Consequently, there are no barriers for electron and hole injection across the interface at the Alq_3/PTCDA heterojunction, whereas there are substantial barriers for both carriers at the Alq_3/α-NPD heterojunction. The Alq_3/α-NPD interface confines electrons in the emissive layer (Alq_3) but also introduces a barrier for hole injection into the emissive layer. The Alq_3/PTCDA interface, on the other hand, favors hole injection into the ET layer but allows electron leakage into the nonemissive layer. Neither case is optimum. These characteristics do explain in part the higher electroluminescent efficiency, presumably due to good electrons confinement in Alq_3, obtained with the Alq_3/α-NPD pair.[20] They are also consistent with the higher turn-on voltage, due to the hole injection barrier, than that achieved with the Alq_3/PTCDA pair.[20] Although other issues like differences in the quality of contacts to PTCDA and α-NPD, and the role of traps in the electron transport in Alq_3 must be taken into account in a complete analysis of the electrical behavior of these interfaces, our measurements indicate that a promising avenue for improving the performance of Alq_3-based heterojunction OLEDs consist in identifying wide gap HT materials with large IE and small EA to achieve a nested ''band structure'' configuration.

With regard to the PTCDA/α-NPD interface, thin layers of PTCDA sandwiched between indium tin oxide (ITO) and α-NPD have been used to improve hole injection in cases where the transparent electrode is deposited on the organic layer.[21] Figure 6(c) shows that the relative HOMO positions are indeed adequate for easy hole injection from PTCDA into α-NPD. Yet, it appears paradoxical that hole injection could be improved by injecting first from ITO into a layer with very high ionization energy. It is believed, however, that the ITO/PTCDA interface is strongly affected by the chemistry between In and PTCDA and that the resulting electronic gap states facilitate the injection of holes.[7,8]

The shift in photoemission onset at Alq_3/PTCDA and Alq_3/α-NPD demonstrates that the widely used assumption of E_{vac} alignment is invalid for these organic-organic interfaces. The photoemission work of Ishii *et al.*[18] on organic-metal interfaces lead to the same general conclusion. The vacuum level rise toward the HT layer corresponds to a negative charge transfer from the ET to the HT layer and formation of an interface dipole. The charge separation is presumably confined to very few molecular layers on each side of the interface. At inorganic heterojunctions, dipoles correspond to the tailing of electron wave functions across the interface and occupation of interface-induced states as a function of electronegativity difference between the two semiconductors.[6] The utility of these concepts, however, has not yet been demonstrated for molecular interfaces. Electrons are considerably more localized in these solids, and surface and interface states, as we know them on inorganic semiconductor surfaces, do not exist on molecular surfaces. We find no interface dipole between PTCDA and α-NPD which exhibit very different IE and EA, and presumably different electronegativity. Furthermore, the directions of the dipole at the Alq_3/PTCDA and Alq_3/α-NPD interfaces are the same, although the signs of the HOMO and LUMO offsets are opposite. It is therefore likely that more local mechanisms, such as changes in molecule conformation in the heterogeneous medium of the interface and ''polarization'' of the weak van der Waals bonds between unlike molecules, are responsible for these interface dipoles.

V. SUMMARY

Using ultraviolet photoemission spectroscopy, we have investigated the formation of three organic-organic heterojunctions between one ET (Alq_3) and two HT (PTCDA and α-NPD) materials and determined their electronic structure. We have measured energy offsets between HOMO levels directly at the interface. We have found that the relative positions of HOMOs and LUMOs across the Alq_3/PTCDA and Alq_3/α-NPD interfaces are qualitatively different and may explain, in part, the different performances of corresponding devices. We have established the existence of substantial charge transfer-induced dipoles at two of these interfaces. These dipoles invalidate previous assumptions of vacuum level alignment across organic heterojunctions. Finally, we have found that the molecular level alignment is independent of the deposition sequence of the organic films and that transitivity applies to these organic ''band offsets.''

ACKNOWLEDGMENTS

Support of this work by the MRSEC program of the National Science Foundation under award number DMR-9400362 is gratefully acknowledged. The authors also thank S. R. Forrest for providing the organic source materials.

[1] For review, see N. C. Greenham and R. H. Friend, *Solid State Physics Series*, edited by H. Ehrenreich and F. Saepen (Academic, New York, (1995), Vol. 48, p. 1; S. R. Forrest, Chem. Rev. **97**, 1793 (1997).
[2] C. W. Tang and S. A. VanSlyke, Appl. Phys. Lett. **51**, 913 (1987).
[3] C. W. Tang, S. A. VanSlyke, and C. H. Chen, J. Appl. Phys. **65**, 3610 (1989).
[4] Z. Shen, P. E. Burrows, V. Bulovic, S. R. Forrest, and M. E. Thompson, Science **276**, 2009 (1997).
[5] P. H. Rieger, *Electrochemistry* (Chapman & Hall, New York, 1994).
[6] For review, see M. Lannoo and P. Friedel, *Atomic and Electronic Structure of Surfaces* (Springer-Verlag, Berlin, 1991); W. Mönch, *Semiconductor Surfaces and Interfaces* (Springer-Verlag, Berlin, 1993).
[7] Y. Hirose, A. Kahn, V. Aristov, and P. Soukiassian, Appl. Phys. Lett. **68**, 217 (1996).
[8] Y. Hirose, A. Kahn, V. Aritov, P. Soukiassian, V. Bulovic, and S. R. Forrest, Phys. Rev. B **54**, 13 748 (1996).
[9] S. Narioka, H. Ishii, D. Yoshimura, M. Sei, Y. Ouchi, K. Seki, S. Hasegawa, T. Miyazaki, Y. Harima, and K. Yamashita, Appl. Phys. Lett. **67**, 1899 (1995).
[10] W. R. Salaneck and J. L. Brédas, Adv. Mater. **8**, 48 (1996).
[11] Y. Park, V. Choong, E. Ettedgui, Y. Gao, B. R. Hsieh, T. Wehrmeister, and K. Müllen, Appl. Phys. Lett. **69**, 1080 (1996).
[12] A. Rajagopal and A. Kahn, Adv. Mater. (accepted for publication).
[13] N. Sato and M. Yoshikawa, J. Electron Spectrosc. Relat. Phenom. **78**, 387 (1996).
[14] Y. Hirose, W. Chen, E. I. Haskal, S. R. Forrest, and A. Kahn, J. Vac. Sci. Technol. B **12**, 2616 (1994).
[15] N. Karl and N. Sato, Mol. Cryst. Liq. Cryst. **218**, 79 (1992).
[16] A. Schmidt, M. L. Anderson, and N. R. Armstrong, J. Appl. Phys. **78**, 5619 (1995).
[17] A. Rajagopal, Y. Hu, and A. Kahn (unpublished).
[18] H. Ishii and K. Seki, IEEE Trans. Electron Devices **44**, 1295 (1997).
[19] C. I. Wu, Y. Hirose, H. Sirringhaus, and A. Kahn, Chem. Phys. Lett. **272**, 43 (1997).
[20] P. E. Burrows and S. R. Forrest, Appl. Phys. Lett. **64**, 2285 (1994).
[21] V. Bulovic, P. Tian, P. E. Burrows, M. R. Gokhale, S. R. Forrest, and M. E. Thompson, Appl. Phys. Lett. **70**, 2954 (1997).